biomedicines

MDPI

*Article*

# SARS-CoV-2 impact on red blood cell morphology

**Kirill A. Kondratov[1,2,3,*], Alexander A. Artamonov[2], Vladimir Yu. Mikhailovskii[3], Anastasiya A. Velmiskina[1,3], Sergey V. Mosenko[1,3], Evgeniy A. Grigoryev[3], Anna Yu. Anisenkova[1,3], Yuri V. Nikitin[2], Svetlana V. Apalko[1,3], Natalya N. Sushentseva[1], Andrey M. Ivanov[2] and Sergey G. Scherbak[1,3].**

1 City Hospital No. 40 St. Petersburg 197706 Russia
2 Military Medical Academy N.a. S.M. Kirov St. Petersburg 194044 Russia
3 Saint-Petersburg State University St. Petersburg 199034 Russia
*kondratovk.kirill@yandex.ru.

**Abstract:** Severe COVID-19 alters the biochemical and morphological characteristics of blood cells in a wide variety of ways. To date, however, the vast majority of research has been devoted to the study of leukocytes, while erythrocyte morphological changes have received significantly less attention. The purpose of this research was to identify erythrocyte types that were unique to COVID-19, compare the number of different poikilocyte types, and measure erythrocyte sizes to provide data on size dispersion. Red blood cells obtained from 6 control donors (800-2200 cells for each donor) and 5 COVID-19 patients (800-1900 cells for each patient) were examined using low voltage scanning electron microscopy. We did not discover any forms of poikilocytes that would be unique to COVID-19. Among COVID-19 patients, we observed an increase in the number of acanthocytes (p=0.01) and a decrease in the number of spherocytes (p=0.03). In addition, our research demonstrates that COVID-19 causes an increase in the median (p=0.004) and interquartile range (p=0.009) when assessing erythrocyte size.

**Keywords:** COVID-19; erythrocyte; red blood cells; cytokine storm; severe COVID-19; low voltage scanning electron microscopy; erythrocyte size

## 1. Introduction

Since the beginning of the pandemic in 2020, COVID-19 has raised many questions regarding our understanding of the immunopathogenesis of viral infections. To date, there is still no common opinion that would unite and explain the changes that occur in the human body during a cytokine storm initiated by sars-cov-2 infection. A significant part of studies by research groups from all around the world are dedicated to researching the immune response to COVID-19 1, often focusing on cytokines, inflammatory markers 2, quantitative and morphological parameters of the immune system 3, 4. Fewer studies make an attempt to analyze red blood cells (RBC), specifically the morphology of erythrocytes in patients undergoing cytokine storm. Given the fact that COVID-19 primarily affects the respiratory system 5, often inducing hypoxia 6 and resulting in conditions that a human becomes vulnerable to during low oxygen saturation, it is probable to assume that COVID-19 can affect the main transporters of O2 in the human body — erythrocytes 7. Our aim was to identify changes that occur in red blood cells during COVID-19 induced cytokine storm, to study RBC morphology using Low-Voltage Scanning Electron Microscopy (LVSEM) images and conduct a comparative RBC morphology analysis between healthy donors and SARS-CoV-2 infected patients.

## 2. Materials and methods

### *2.1. Patients and data collection*

A total of 11 research participants were divided into 2 groups: 5 COVID-19 patients and 6 healthy donors. Our control group consisted of 6 healthy donors (mean age 51).

The 5 COVID-19 patients (mean age 67) presented to our hospital from April 1st, 2022, to August 23rd, 2022. All patients were laboratory confirmed to be SARS-CoV-2 infected by real-time RT-PCR. Three patients were admitted to the intensive care unit, and two in the infectious disease unit. Severe patients were admitted to the ICU according to our national clinical guidelines as follows: body temperature ≥ 39ºC, Respiratory Rate ≥ 30/min, oxygen saturation (SpO2) ≤ 93%.

### *2.2. Blood sample preparation*

Fasting whole blood from every patient was collected aseptically by venipuncture into ethylenediamine tetraacetic acid (EDTA) collection tubes on the 4th day of hospital admission. Whole blood was centrifuged at 1500 g for 10 minutes, the supernatant was extracted after. 2 μl of cell pellet was added to 5 ml phosphate-buffered saline. Centrifuged at 1000 g for 10 minutes. Extracted the supernatant, added 500 μl of phosphate-buffered saline to the pellet. Sample preparation for LVSEM was performed according to a standardized protocol as previously described [8].

### *2.3. Low voltage scanning electron microscopy for erythrocyte size evaluation. Technique Description.*

Further examination was carried out on a Zeiss Merlin Scanning Electron Microscope, 1.00 KX magnification in High Resolution mode, EHT 0.400 kV. We analyzed 10 fields of view that corresponded to 10 LVSEM images.

The Feret diameter was chosen as the main parameter for erythrocyte size evaluation.

We measured the feret diameter of erythrocytes in ImageJ2. (Version 1.54b 08 January 2023). The scale was calibrated according to the LVSEM image micrometer ruler. Known 10 μm (micrometers) corresponds to 137.75 pixels in all images with resolution 3072x2304. Global scaling was applied. To perform a standardized count of the Feret's diameter of erythrocytes of control and COVID-19 patients, we programmed a macro to execute an automated analyzation process. As a result of the analyze particles process and the show overlay masks function we received a picture for every LVSEM image with contours of counted erythrocytes, separation lines of adjacent cells, counts of the number of erythrocytes, the diameter of each cell, the minimum Feret diameter, and the erythrocyte area. The values for each cell were recorded in a database table and used for further statistical analysis.

### *2.4. Erythrocyte morphology study*

For quantifying and presenting pathologic forms of erythrocytes in charts we introduced a strict selection criteria:

-Echinocytes - presence of three or more evenly spread spike-like protrusions of plasmalemma on membrane surface with length varying from 0.5 to 2 μm with wide base, the angle between the apical part of the spike and the surface of the echinocyte membrane is usually in the range from 100 to 130 degrees. The end sections of the spikes form an acute angle.

-Acanthocytes - presence of irregularly distributed plasmalemma protrusions in the form of spines, including single ones, from 2 μm in length. The end sections of the spines end with a club-shaped extension at the apical end. The size and shape of the spines on a single acanthocyte may vary and have no strict pattern of distribution on the membrane surface.

-Stomatocytes - increased volume compared to normocytes by 20-30% and deep slit-shaped central lumen, which on the opposite side forms a semi-oval convexity with a smooth surface. The size of the central lumen depends on the degree of crenulation and

can range from wide funnel-shaped to slit-shaped. Because of the strong roundness of one of the sides, they lie on their sides and are usually easily detected.

-Ovalocytes are oval or elongated erythrocytes from ovoid to bacilliform or pencil shape. The central lumen is flattened, may not be defined. The end sections of the cells are blunt, and the membrane is smooth.

-Spherocytes are erythrocytes that have lost their biconcave shape. Spherocytes are globular in shape and lack a central lumen or depression, which is most clearly visible under light microscopy.

-Schistocytes - erythrocytes are separated into fragments 2 to 3 μm in diameter. The usual round shape is absent; instead, they have a triangular or other angular morphology. Schistocytes are also classified as any degenerately altered irregularly shaped cells not conforming to other known shapes. The central lumen zone is often absent.

-Degmacytes - a bitten cell - the cell looks as if it has been bitten. has a semicircular depression on the outer side of the membrane.

-Tear cells (dacryocytes) are drop-shaped or pear-shaped erythrocytes with one large spicule with a blunt end. Cell size varies. 9, 10.

For counting pathologic forms of erythrocytes we used the Cell Counter plugin for ImageJ/Fiji by Kurt de Vos 11, in which we designated 8 groups of poikilocytes as mentioned above. For counting pathologic forms we used the same images that we analyzed for measuring the size of erythrocytes.

### *2.5. Statistical analysis*

Statistical analysis was performed in RStudio (version 2022.12.0+353.pro3). Statistical analysis for the results was executed by applying Wilcoxon-Mann-Whitney test. A p-value $<0.05$ was considered statistically significant. Median value, interquartile range is presented graphically. Data visualization, images and charts were made with RStudio tidyverse, ggplot2 and sinaplot open-source packages

## **3. Results**

### *3.1. Erythrocyte morphology study*

We performed a comparative analysis of pathologic forms found in COVID-19 patients (Fig 2) and healthy donors (Fig 1). We did not observe any unique pathologic forms.

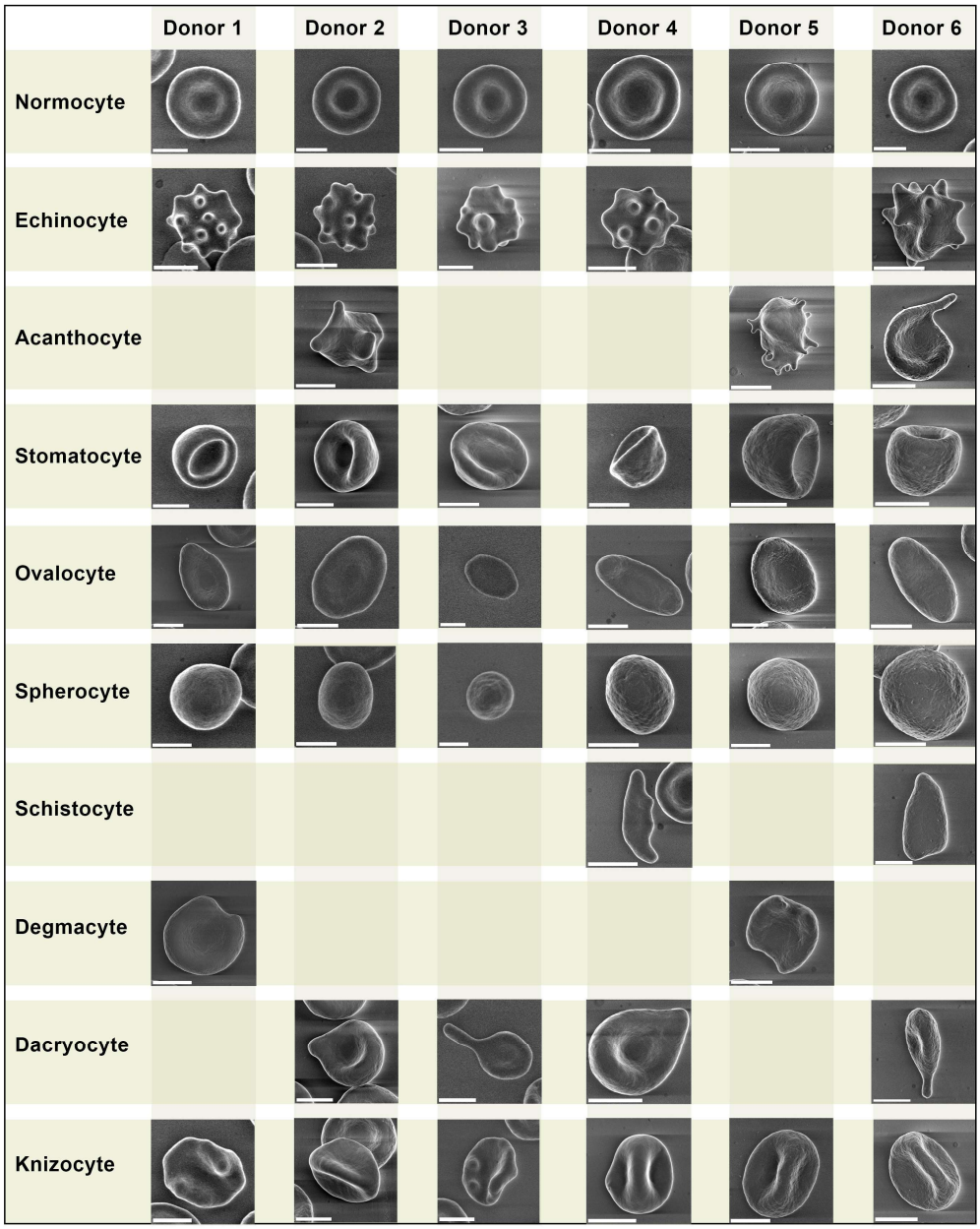


**Figure 1.** Morphological types of erythrocytes of six control donors. Images obtained by LVSEM. White segment is equal to 1 μm.

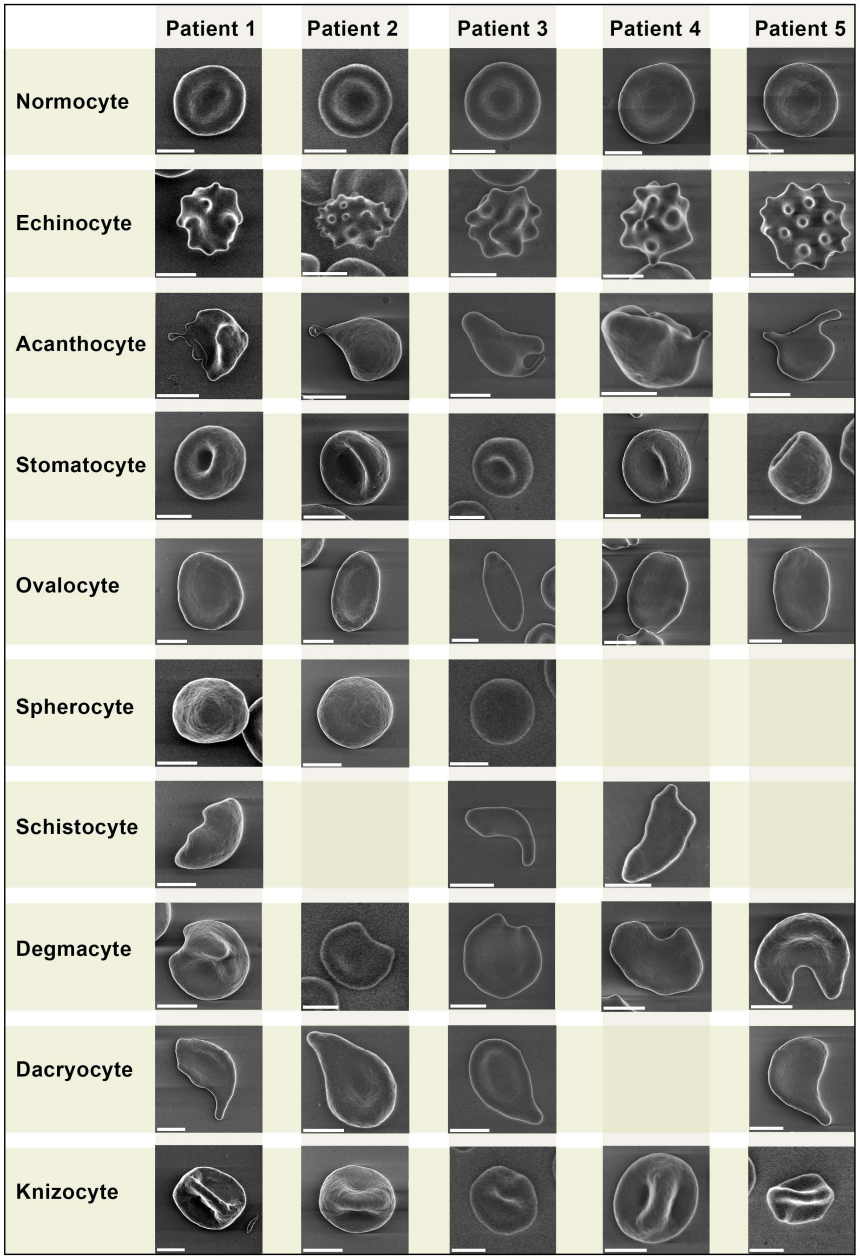


.

**Figure 2.** Morphological types of erythrocytes of five patients with severe COVID-19. Images obtained by LVSEM. White segment is equal to 1 μm.

Despite being similar, some pathologic forms, in particularly acanthocytes of COVID-19 patients, exhibited more pronounced plasmalemma protrusion. Acanthocytes were found in blood samples of all 5 COVID-19 patients, while in healthy donors they were found sporadically in only 3 samples. Overall, we did not find any significant differences in erythrocyte morphology between healthy donors and COVID-19 patients.

We present a comparative grid chart with images of normocytes and poikilocytes that we acquired from our blood samples. Blank grids denote cells that were not present.

*3.2. Poikilocyte percentage count*

At the next step we used the same images to count pathological forms of erythrocytes according to the criteria that we designated earlier in materials and methods (Fig 3). The

difference between the overall number of poikilocytes in healthy donors and COVID-19 patients was insignificant, 873 and 919 respectively. We found an increase in the percentage of acanthocytes among COVID-19 patients in comparison with healthy donors. Other significant data worth noting were the raised percentages of spherocytes in healthy donors.

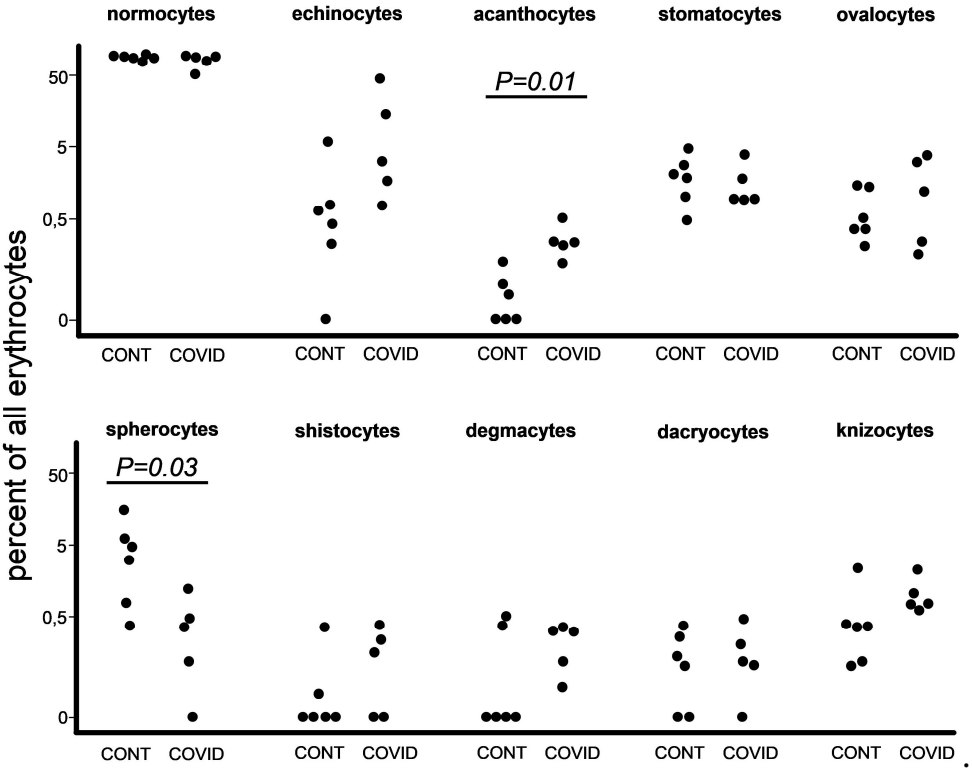


**Figure 3.** Comparison of the proportions of distinct morphological erythrocyte types (normocytes and other forms of poikilocytes) in control donors and patients with severe COVID-19.

### *3.3. Erythrocyte size evaluation*

After processing the LVSEM images we evaluated the size of erythrocytes (Fig 4) by the method described above (materials & methods). Each sample contained between 1200 to 2270 erythrocytes. We have noted that there is a reliable increase in median (Fig 4, panel b) and interquartile range erythrocyte size in the COVID-19 group in comparison to healthy donors.

A

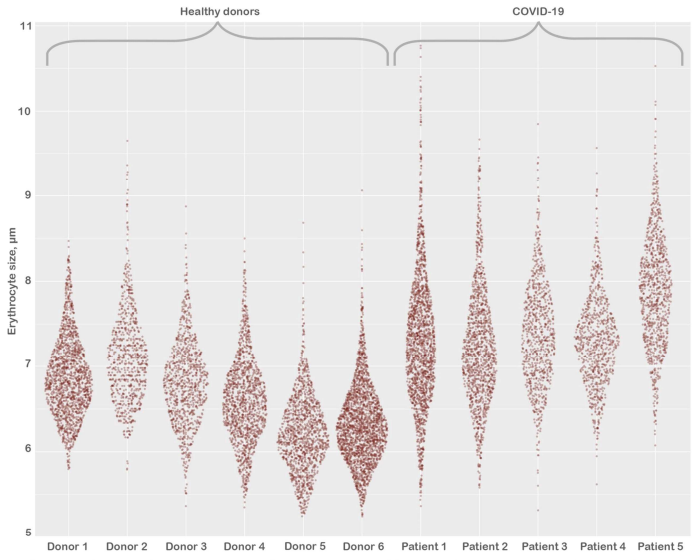


B

| | Donor 1 | Donor 2 | Donor 3 | Donor 4 | Donor 5 | Donor 6 | Patient 1 | Patient 2 | Patient 3 | Patient 4 | Patient 5 | |
|---|---|---|---|---|---|---|---|---|---|---|---|---|
| Median, µm | 6,835 | 7,097 | 6,794 | 6,568 | 6,181 | 6,286 | 7,252 | 7,154 | 7,349 | 7,282 | 7,893 | *p = 0,004* |
| *Interquartile range* | 0,604 | 0,692 | 0,642 | 0,623 | 0,554 | 0,562 | 0,958 | 0,844 | 0,821 | 0,666 | 0,886 | *p = 0,009* |

**Figure 4.** Comparison of erythrocyte sizes from six control donors and five patients with severe COVID-19 Pannel A. Erythrocyte size distribution. Pannel B. Comparison of median and interquartile range of RBC size samples.

## 4. Discussion

The impact of SARS-CoV 2 on red blood cells is still not clearly defined. Due to the fact that the overwhelming majority of research since the beginning of the COVID-19 pandemic is dedicated to studying immunological parameters 2, 12, to date there is little data to rely on statistically.

The significant set of features that we found during our study can potentially be reflected in a number of conditions not associated with SARS-CoV-2 infection.

We did not observe any unique pathologic forms (Fig. 1, Fig. 2) similar to the mushroom-shaped cells described by Gérard. D et al. 13. It should be emphasized that the vast majority of research on poikilocytosis, both in COVID-19 and in other diseases, use light microscopy to evaluate aberrant erythrocyte shapes. By employing the LVSEM method in our study, we observed precise cell morphology. However, the criteria for isolating diverse types of poikilocytes change when erythrocytes are examined using this approach. Specifically, due to the opacity of cells, the location of the cell on the substrate is crucial while monitoring erythrocytes using LVSEM. In example, a disoriented stomatocyte with its invagination pointing toward the substrate will appear as a spherocyte. Therefore, comparing our findings to that obtained from light microscopy-based examination of poikilocytes is not completely accurate. It should also be noted that patients with pre-existing diseases are significantly more likely to experience a severe course of COVID-19, therefore any changes in erythrocyte size and the ratio of morphology deviations between the two study groups may be caused by this.

We observed a rise in acanthocyte percentage (Fig. 3). The formation of acanthocytes is commonly associated with conditions such as severe liver dysfunction, neuroacanthocytosis, abetalipoproteinemia 14, malnutrition, hypothyroidism, post-splenectomy conditions 15. Alterations in membrane lipids or structural proteins remain as the leading causes of acanthocyte formation 16. Liver dysfunction leads to the accumulation of, apolipoprotein A-II deficient lipoprotein in plasma causing increased cholesterol in RBCs. This causes abnormalities of membrane of RBC causing remodeling in spleen and formation of acanthocytes. In abetalipoproteinemia, there is a deficiency of lipids and vitamin E causing abnormal morphology of RBCs 17.

It is worth noting that most of the aforementioned conditions are associated with either protein or lipid disorders, both of which are a risk factor in COVID-19 infection 18, 19.

We have no exact explanation on why the percentage of spherocytes was lower among COVID-19 patients in our study (Fig 3). We can also assume that during pyrexia, cytokine storm, and general immune hyperreactivity spherocytes undergo elimination by splenic and liver macrophages 20, 21 at a more rapid rate, therefore leading to a decrease of spherocyte presence in peripheral blood of COVID-19 patients.

Our remarkable findings of significant increase in erythrocyte size (Fig 4, pannel B) coincide with the studies of several research groups if extrapolated to red cell distribution width (RDW). Lippi, Giuseppe et al. state that the absolute RDW-CV value was higher in COVID-19 patients with severe illness compared to those with mild disease 22. Marchi, Giacomo et al. also confirm higher (RDW) levels in the group with elevated RBCs alterations 23. Karampitsakos, Theodoros et al. state that values of RDW ≥14.5% were also strongly associated with increased risk of mortality 24.

In order to elucidate our observations and their possible interrelations with similar findings of other research groups, we propose 3 possible pathogenetic pathways that could lead to the aforementioned RBC abnormalities:

S.Valsami al. 25 concluded that SARS-CoV-2 infection has an effect on RBC and that there seems to be an association between RBC markers and disease severity in their study. They report elevated hemolysis markers, specifically Lactate-dehydrogenase and plasma free-Hemoglobin. However, our patients did not exhibit any clinical or laboratory manifestations of hemolysis 26, 27. It is probable that this process was latent and could be observed only in later stages of the clinical onset. Valsami et al. also state that COVID-19 patients' RBCs were more sensitive to mechanical stress, and exhibited significantly elevated apoptotic markers (iCa2+, phosphatidylserine RBC-PS) 25. Nguyen, Duc Bach et al. 28 confirm in their study that an increased intracellular Ca2+ content of RBCs results in the activation of several processes, important for phosphatidylserine exposure, eventually leading to loss of KCl and water, causing cell shrinkage, cytoskeleton destruction, membrane blebbing, and micro-vesiculation. Hoffman, Joseph F et al. 29 also state that the Ca2+-activated K+ channel (Gardos channel) represents the major pathway for cell shrinkage via KCl and water loss. Qadri, Syed M et al. 30 and Föller, Michael et al. 31 state that cell stressors such as hypertonic shock, energy deprivation, and increased temperature may result in the activation of the aforementioned channels, which coincides with the conditions that our COVID-19 patients were experiencing. Remarkably, we found no evident signs of the aforementioned cell shrinkage. We assume that Cytoskeleton destruction manifested itself in the form of poikilocytes that were almost equally presented in healthy donors and COVID-19 patients.

Another possible pathogenetic mechanism is COVID-19-associated coagulopathy, the formation of microvascular thrombi and direct physical RBC damage. This theory is commonly spread due to the well-known pathogenetic mechanisms of SARS-CoV-2 ability to infect type II pneumocytes via angiotensin-converting enzyme 2 (ACE2) 32, cells that are in direct apposition to the alveolar vascular network leading to diffuse microvascular thrombosis 33 and high incidence of major thrombotic events in patients with COVID-19 34. Contrary to this data, we did not find any tracks of coagulopathy on a microscopic level such as rouleaux formations or signs of autoagglutination 34.

Plassmeyer, Matthew et al. state that they observed elevated caspase-3/7 levels in red blood cells in COVID-19 patients compared to controls 35. It is known that the development and differentiation of erythroid progenitor cells might be regulated through caspase-dependent apoptosis 36, 37. Graeme W. Carlile, Deborah H. Smith, Martin Wiedmann in an ex vivo experiment proved that during erythropoiesis cells that received caspase-3 siRNA were arrested at the pronormoblast stage. In the control, virtually all of the pronormoblasts were able to progress to basophilic normoblasts while in the siRNA-treated culture a fraction of the pronormoblasts were blocked in development. 50% of the

siRNA-treated culture remained as pronormoblasts by day 17 of the experiment 38. Zermati, Y et al. state that caspase inhibitors arrest erythroid development in human cells 39.

This data suggests that caspases play a key role in erythropoiesis, which leads us to a hypothesis that the elevated presence of caspase-3/7 in the RBC of COVID-19 patients 35 could be the result of immature forms entering the bloodstream. This hypothesis elucidates our findings of significant increase in erythrocyte size. A recent study shows that RBC precursors express ACE2 receptor at day 5 of differentiation 40. SARS-CoV-2, as said earlier 32, has an increased affinity for the ACE2 receptor, therefore making RBC precursors a direct target for viral infection, leading to significant iron dysmetabolism and disturbances of oxygen-binding capacity in severely ill COVID-19 patients 40, thereby exacerbating hypoxia. Systemic hypoxia induced by low oxygen saturation leads to upregulated production of erythropoietin by peritubular cells of the kidney 41. Bapat, Aditi et al. state that hypoxia promotes erythroid differentiation by supporting the maintenance of progenitor populations and enhancing the formation of proerythroblasts and also significantly accelerates maturation of erythroid cells 42. Vlaski, Marija et al. and Rogers, Heather M et al. also acknowledge that low O2 concentration accelerates erythrocyte proliferation and differentiation 43, 44.

It is well known that after each stage of cell differentiation the erythrocyte reduces in size 45. Given the fact that erythropoiesis takes up to 7 days 46, and that our patients' blood samples were taken on the 4th day after hospital admission, it is possible that the significant increase in erythrocyte size is due to the prevalence of immature forms of erythrocytes in COVID-19 patients' blood samples. This theory could also complement the findings of Plassmeyer, Matthew et al. mentioned earlier 35.

## 5. Conclusion:

Using low-voltage scanning electron microscopy, in our research we demonstrate that severe COVID-19 causes an increase in the size and dispersion of erythrocytes, the number of acanthocytes, and a decrease in the number of spherocytes.

**Supplement material:** The following supporting information can be downloaded at: www.mdpi.com/xxx/s1, Table S1: www.mdpi.com/xxx/s2 Erythrocyte types; Table S2 Erythrocyte size.

**Funding:** This work was supported by Saint Petersburg State University, project ID: 94029859. The investigation of the structure by means low-voltage scanning electron microscopy was carried out at the IRC for Nanotechnology of the Science Park of St. Petersburg State University within the framework of project No. AAAA-A19-119091190094.

**Institutional Review Board Statement:** This study was conducted according to the guidelines of the declaration of Helsinki and approved by the Ethics Committee.

**Informed Consent Statement:** Informed consent was obtained from all subjects involved in the study.

**Data Availability Statement:** The results of size calculations and number of different forms of erythrocytes are presented in the Supplement material. All micrographs of erythrocytes obtained during the research can be provided at the first request sent to kondratovk.kirill@yandex.ru

**Conflicts of Interest:** The authors declare no conflict of interest.

## References

1. Boechat, J.L.; Chora, I.; Morais, A.; Delgado, L. The Immune Response to SARS-CoV-2 and COVID-19 Immunopathology – Current Perspectives. *Pulmonology* **2021**, *27*, 423–437, doi:10.1016/j.pulmoe.2021.03.008.
2. Lucas, C.; Wong, P.; Klein, J.; Castro, T.B.R.; Silva, J.; Sundaram, M.; Ellingson, M.K.; Mao, T.; Oh, J.E.; Israelow, B.; et al. Longitudinal Analyses Reveal Immunological Misfiring in Severe COVID-19. *Nature* **2020**, *584*, 463–469, doi:10.1038/s41586-020-2588-y.

3. Nikitin Yu.V., Aleksandrova E.V., Krivoruchko A.B., Meshkova M.E., Minaeva L.V., Zhdanov K.V., Artamonov A.A., Kozlov K.V., Ivanov A.M., Maltsev O.V., Ivanov K.S., Lyashenko Yu.I., Masalov E.B. Interrelations between viral load and cellular immunity in patients with COVID-19 of varying severity. *Medical Immunology (Russia)*. **2023**, *25*, 167–180, doi:10.15789/1563-0625-IBV-2586.
4. Lee, C.-T.; Teo, W.Z.Y. Peripheral Blood Smear Demonstration of Lymphocyte Changes in Severe COVID-19. *The American Journal of Tropical Medicine and Hygiene* **2020**, *103*, 1350–1351, doi:10.4269/ajtmh.20-0721.
5. Rahimi, B.; Vesal, A.; Edalatifard, M. Coronavirus and Its Effect on the Respiratory System: Is There Any Association between Pneumonia and Immune Cells. *J Family Med Prim Care* **2020**, *9*, 4729–4735, doi:10.4103/jfmpc.jfmpc_763_20.
6. Nitsure, M.; Sarangi, B.; Shankar, G.H.; Reddy, V.S.; Walimbe, A.; Sharma, V.; Prayag, S. Mechanisms of Hypoxia in COVID-19 Patients: A Pathophysiologic Reflection. *Indian J Crit Care Med* **2020**, *24*, 967–970, doi:10.5005/jp-journals-10071-23547.
7. Kuhn, V.; Diederich, L.; Keller, T.C.S.; Kramer, C.M.; Lückstädt, W.; Panknin, C.; Suvorava, T.; Isakson, B.E.; Kelm, M.; Cortese-Krott, M.M. Red Blood Cell Function and Dysfunction: Redox Regulation, Nitric Oxide Metabolism, Anemia. *Antioxid Redox Signal* **2017**, *26*, 718–742, doi:10.1089/ars.2016.6954.
8. Fedorov, A.; Kondratov, K.; Kishenko, V.; Mikhailovskii, V.; Kudryavtsev, I.; Belyakova, M.; Sidorkevich, S.; Vavilova, T.; Kostareva, A.; Sirotkina, O.; et al. Application of High-Sensitivity Flow Cytometry in Combination with Low-Voltage Scanning Electron Microscopy for Characterization of Nanosized Objects during Platelet Concentrate Storage. *Platelets* **2020**, *31*, 226–235, doi:10.1080/09537104.2019.1599337.
9. Bessis, M. Red Cell Shapes. An Illustrated Classification and Its Rationale. *Nouv Rev Fr Hematol* **1972**, *12*, 721–745.
10. Karandeniya, D.M.W.; Holmes, D.W.; Sauret, E.; Gu, Y.T. A New Membrane Formulation for Modelling the Flow of Stomatocyte, Discocyte, and Echinocyte Red Blood Cells. *Biomech Model Mechanobiol* **2022**, *21*, 899–917, doi:10.1007/s10237-022-01567-4.
11. O'Brien, J.; Hayder, H.; Peng, C. Automated Quantification and Analysis of Cell Counting Procedures Using ImageJ Plugins. *JoVE* **2016**, 54719, doi:10.3791/54719.
12. Merad, M.; Blish, C.A.; Sallusto, F.; Iwasaki, A. The Immunology and Immunopathology of COVID-19. *Science* **2022**, *375*, 1122–1127, doi:10.1126/science.abm8108.
13. Gérard, D.; Ben Brahim, S.; Lesesve, J.F.; Perrin, J. Are Mushroom-shaped Erythrocytes an Indicator of COVID-19? *Br J Haematol* **2021**, *192*, 230–230, doi:10.1111/bjh.17127.
14. Boltshauser, E.; Weber, K.P. Laboratory Investigations. In *Handbook of Clinical Neurology*; Elsevier, 2018; Vol. 154, pp. 287–298 ISBN 978-0-444-63956-1.
15. Naeim, F.; Nagesh Rao, P.; Song, S.X.; Grody, W.W. Disorders of Red Blood Cells—Anemias. In *Atlas of Hematopathology*; Elsevier, 2013; pp. 675–704 ISBN 978-0-12-385183-3.
16. Pacheco, J.M.; Yilmaz, M.; Rice, L. How Low Is Too Low: Statin Induced Hemolysis. *Am. J. Hematol.* **2016**, *91*, 267–267, doi:10.1002/ajh.24105.
17. Lausch, E.; Yoshimi, A. Acanthocytosis: A Key Feature for the Diagnosis of Abetalipoproteinemia. *Blood* **2023**, *141*, 3231–3231, doi:10.1182/blood.2023020260.
18. Loosen, S.H.; Jensen, B.-E.O.; Tanislav, C.; Luedde, T.; Roderburg, C.; Kostev, K. Obesity and Lipid Metabolism Disorders Determine the Risk for Development of Long COVID Syndrome: A Cross-Sectional Study from 50,402 COVID-19 Patients. *Infection* **2022**, *50*, 1165–1170, doi:10.1007/s15010-022-01784-0.
19. Jin, H.; He, J.; Dong, C.; Li, B.; Ma, Z.; Li, B.; Huang, T.; Fan, J.; He, G.; Zhao, X. Altered Lipid Profile Is a Risk Factor for the Poor Progression of COVID-19: From Two Retrospective Cohorts. *Frontiers in Cellular and Infection Microbiology* **2021**, *11*.
20. Klei, T.R.L.; Meinderts, S.M.; Van Den Berg, T.K.; Van Bruggen, R. From the Cradle to the Grave: The Role of Macrophages in Erythropoiesis and Erythrophagocytosis. *Front. Immunol.* **2017**, *8*, doi:10.3389/fimmu.2017.00073.
21. Thiagarajan, P.; Parker, C.J.; Prchal, J.T. How Do Red Blood Cells Die? *Front. Physiol.* **2021**, *12*, 655393, doi:10.3389/fphys.2021.655393.
22. Lippi, G.; Henry, B.M.; Sanchis-Gomar, F. Red Blood Cell Distribution Is a Significant Predictor of Severe Illness in Coronavirus Disease 2019. *Acta Haematol* **2021**, *144*, 360–364, doi:10.1159/000510914.
23. Marchi, G.; Bozzini, C.; Bertolone, L.; Dima, F.; Busti, F.; Castagna, A.; Stranieri, C.; Fratta Pasini, A.M.; Friso, S.; Lippi, G.; et al. Red Blood Cell Morphologic Abnormalities in Patients Hospitalized for COVID-19. *Front Physiol* **2022**, *13*, 932013, doi:10.3389/fphys.2022.932013.
24. Karampitsakos, T.; Akinosoglou, K.; Papaioannou, O.; Panou, V.; Koromilias, A.; Bakakos, P.; Loukides, S.; Bouros, D.; Gogos, C.; Tzouvelekis, A. Increased Red Cell Distribution Width Is Associated With Disease Severity in Hospitalized Adults With SARS-CoV-2 Infection: An Observational Multicentric Study. *Front Med (Lausanne)* **2020**, *7*, 616292, doi:10.3389/fmed.2020.616292.
25. Bouchla, A.; Kriebardis, A.G.; Georgatzakou, H.T.; Fortis, S.P.; Thomopoulos, T.P.; Lekkakou, L.; Markakis, K.; Gkotzias, D.; Panagiotou, A.; Papageorgiou, E.G.; et al. Red Blood Cell Abnormalities as the Mirror of SARS-CoV-2 Disease Severity: A Pilot Study. *Front. Physiol.* **2022**, *12*, 825055, doi:10.3389/fphys.2021.825055.
26. Ballas, S.K. Lactate Dehydrogenase and Hemolysis in Sickle Cell Disease. *Blood* **2013**, *121*, 243–244, doi:10.1182/blood-2012-10-462135.

27. Berlin, N.; Berk, P. Quantitative Aspects of Bilirubin Metabolism for Hematologists. *Blood* **1981**, *57*, 983–999, doi:10.1182/blood.V57.6.983.983.
28. Nguyen, D.B.; Wagner-Britz, L.; Maia, S.; Steffen, P.; Wagner, C.; Kaestner, L.; Bernhardt, I. Regulation of Phosphatidylserine Exposure in Red Blood Cells. *Cellular Physiology and Biochemistry* **2011**, *28*, 847–856, doi:10.1159/000335798.
29. Hoffman, J.F.; Joiner, W.; Nehrke, K.; Potapova, O.; Foye, K.; Wickrema, A. The HSK4 (KCNN4) Isoform Is the Ca2+-Activated K+ Channel (Gardos Channel) in Human Red Blood Cells. *Proc Natl Acad Sci U S A* **2003**, *100*, 7366–7371, doi:10.1073/pnas.1232342100.
30. Qadri, S.M.; Bissinger, R.; Solh, Z.; Oldenborg, P.-A. Eryptosis in Health and Disease: A Paradigm Shift towards Understanding the (Patho)Physiological Implications of Programmed Cell Death of Erythrocytes. *Blood Rev* **2017**, *31*, 349–361, doi:10.1016/j.blre.2017.06.001.
31. Föller, M.; Braun, M.; Qadri, S.M.; Lang, E.; Mahmud, H.; Lang, F. Temperature Sensitivity of Suicidal Erythrocyte Death. *Eur J Clin Invest* **2010**, *40*, 534–540, doi:10.1111/j.1365-2362.2010.02296.x.
32. Abassi, Z.; Higazi, A.A.R.; Kinaneh, S.; Armaly, Z.; Skorecki, K.; Heyman, S.N. ACE2, COVID-19 Infection, Inflammation, and Coagulopathy: Missing Pieces in the Puzzle. *Front. Physiol.* **2020**, *11*, 574753, doi:10.3389/fphys.2020.574753.
33. Conway, E.M.; Mackman, N.; Warren, R.Q.; Wolberg, A.S.; Mosnier, L.O.; Campbell, R.A.; Gralinski, L.E.; Rondina, M.T.; Van De Veerdonk, F.L.; Hoffmeister, K.M.; et al. Understanding COVID-19-Associated Coagulopathy. *Nat Rev Immunol* **2022**, *22*, 639–649, doi:10.1038/s41577-022-00762-9.
34. Berzuini, A.; Bianco, C.; Migliorini, A.C.; Maggioni, M.; Valenti, L.; Prati, D. Red Blood Cell Morphology in Patients with COVID-19-Related Anaemia. *Blood Transfusion* **2020**, 34–36, doi:10.2450/2020.0242-20.
35. Plassmeyer, M.; Alpan, O.; Corley, M.J.; Premeaux, T.A.; Lillard, K.; Coatney, P.; Vaziri, T.; Michalsky, S.; Pang, A.P.S.; Bukhari, Z.; et al. Caspases and Therapeutic Potential of Caspase Inhibitors in Moderate–Severe SARS-CoV-2 Infection and Long COVID. *Allergy* **2022**, *77*, 118–129, doi:10.1111/all.14907.
36. Berg, C.P.; Engels, I.H.; Rothbart, A.; Lauber, K.; Renz, A.; Schlosser, S.F.; Schulze-Osthoff, K.; Wesselborg, S. Human Mature Red Blood Cells Express Caspase-3 and Caspase-8, but Are Devoid of Mitochondrial Regulators of Apoptosis. *Cell Death Differ* **2001**, *8*, 1197–1206, doi:10.1038/sj.cdd.4400905.
37. Gregoli, P.A.; Bondurant, M.C. Function of Caspases in Regulating Apoptosis Caused by Erythropoietin Deprivation in Erythroid Progenitors. *J Cell Physiol* **1999**, *178*, 133–143, doi:10.1002/(SICI)1097-4652(199902)178:2<133::AID-JCP2>3.0.CO;2-5.
38. Carlile, G.W.; Smith, D.H.; Wiedmann, M. Caspase-3 Has a Nonapoptotic Function in Erythroid Maturation. *Blood* **2004**, *103*, 4310–4316, doi:10.1182/blood-2003-09-3362.
39. Zermati, Y.; Garrido, C.; Amsellem, S.; Fishelson, S.; Bouscary, D.; Valensi, F.; Varet, B.; Solary, E.; Hermine, O. Caspase Activation Is Required for Terminal Erythroid Differentiation. *The Journal of Experimental Medicine* **2001**, *193*, 247–254, doi:10.1084/jem.193.2.247.
40. Kronstein-Wiedemann, R.; Stadtmüller, M.; Traikov, S.; Georgi, M.; Teichert, M.; Yosef, H.; Wallenborn, J.; Karl, A.; Schütze, K.; Wagner, M.; et al. SARS-CoV-2 Infects Red Blood Cell Progenitors and Dysregulates Hemoglobin and Iron Metabolism. *Stem Cell Rev Rep* **2022**, *18*, 1809–1821, doi:10.1007/s12015-021-10322-8.
41. Schoener, B.; Borger, J. Erythropoietin Stimulating Agents. In *StatPearls*; StatPearls Publishing: Treasure Island (FL), 2023.
42. Bapat, A.; Schippel, N.; Shi, X.; Jasbi, P.; Gu, H.; Kala, M.; Sertil, A.; Sharma, S. Hypoxia Promotes Erythroid Differentiation through the Development of Progenitors and Proerythroblasts. *Exp Hematol* **2021**, *97*, 32-46.e35, doi:10.1016/j.exphem.2021.02.012.
43. Vlaski, M.; Lafarge, X.; Chevaleyre, J.; Duchez, P.; Boiron, J.-M.; Ivanovic, Z. Low Oxygen Concentration as a General Physiologic Regulator of Erythropoiesis beyond the EPO-Related Downstream Tuning and a Tool for the Optimization of Red Blood Cell Production Ex Vivo. *Exp Hematol* **2009**, *37*, 573–584, doi:10.1016/j.exphem.2009.01.007.
44. Rogers, H.M.; Yu, X.; Wen, J.; Smith, R.; Fibach, E.; Noguchi, C.T. Hypoxia Alters Progression of the Erythroid Program. *Exp Hematol* **2008**, *36*, 17–27, doi:10.1016/j.exphem.2007.08.014.
45. Sankaran, V.G.; Ludwig, L.S.; Sicinska, E.; Xu, J.; Bauer, D.E.; Eng, J.C.; Patterson, H.C.; Metcalf, R.A.; Natkunam, Y.; Orkin, S.H.; et al. Cyclin D3 Coordinates the Cell Cycle during Differentiation to Regulate Erythrocyte Size and Number. *Genes Dev* **2012**, *26*, 2075–2087, doi:10.1101/gad.197020.112.
46. Jelkmann, W. Regulation of Erythropoietin Production. *J Physiol* **2011**, *589*, 1251–1258, doi:10.1113/jphysiol.2010.195057.